ELSEVIER

Remote Sensing of Environment 82 (2002) 322–334

Remote Sensing of Environment

www.elsevier.com/locate/rse

Automated tree crown detection and delineation in high-resolution digital camera imagery of coniferous forest regeneration

D.A. Pouliot [a], D.J. King [a,*], F.W. Bell [b], D.G. Pitt [c]

[a] *Department of Geography, Carleton University, 1125 Colonel By Drive, Ottawa, Ontario, Canada K1S 5B6*
[b] *Ontario Forest Research Institute, Ontario Ministry of Natural Resources, 1235 Queen Street East, Sault Ste. Marie, Ontario, Canada P6A 2E5*
[c] *Canadian Forest Service, Great Lakes Forestry Centre, P.O. Box 490, Sault Ste. Marie, Ontario, Canada P6A 5M7*

Received 2 November 2001; received in revised form 21 March 2002; accepted 30 March 2002

Abstract

Ensuring successful forest regeneration requires an effective monitoring program to collect information regarding the status of young crop trees and nearby competing vegetation. Current field-based assessment methodology provides the needed information, but is costly, and therefore assessment frequency is low. This often allows undesirable forest structures to develop that do not coincide with management objectives. Remote sensing techniques provide a potentially low-cost alternative to field-based assessment, but require the development of methods to easily and accurately extract the required information. Automated tree detection and delineation algorithms may be an effective means to accomplish this task. In this study, a tree detection–delineation algorithm designed specifically for high-resolution digital imagery of 6-year-old trees is presented and rigorously evaluated. The algorithm is based on the analysis of local transects extending outward from a potential tree apex. The crown boundary is estimated using the point of maximum rate of change in the transect data and a rule base is applied to ensure that the point is contextually suitable. This transect approach is implemented in both the tree-detection and crown-delineation phases. The tree-detection algorithm refines the results of an initial local maximum filter by providing an outline for each detected tree and retaining only one local maximum value within this outline. The crown-delineation algorithm is similar to the detection algorithm, but applies a different rule set in creating a more detailed crown outline. Results show that the algorithm's tree-detection accuracy was better than that using commonly applied fixed-window local maximum filters; it achieved a best result of 91%. For the crown-delineation algorithm, measured diameters from delineated crowns were within 17.9% of field measurements of diameter at the crown base on an individual tree basis and within 3% when averaged for the study. Tests of image pixel spacings from 5 to 30 cm showed that tree-detection accuracy was stable except at the lowest (30-cm) resolution where errors were unacceptable. Delineated crown-diameter accuracy was more sensitive to image resolution, decreasing consistently and nonlinearly with increasing pixel spacing. These results highlight the need for very high resolution imagery in automated object-based analysis of forest regeneration.

1. Introduction

Successful regeneration of coniferous species is critical to forest sustainability in boreal regions. Conifers are the dominant species in this biome, but can be difficult to reestablish after disturbance due to slow growth and sensitivity to competing vegetation. Timely information regarding their stocking levels, health, and competing species abundance is required for effective treatment decisions. Current field-survey methods are labour intensive and costly, resulting in low sample coverage and frequency. As a consequence, undesirable forest structures can develop between sampling periods that are difficult to restore to desired conditions. Remote sensing has potential to provide, at lower cost, forest information with greater coverage than is attainable using field sampling. Early work in the development of remote sensing methods for regeneration assessment focused on manual analysis of large-scale photography (LSP). Results have shown that reliable estimates of stocking, species, crown area, health condition, and stratification of key vegetation complexes can be made (Goba, Pala, & Narraway, 1982; Hall, 1984; Hall & Aldred, 1992; Pitt & Glover, 1993; Pitt, Runesson, & Bell, 2000). However, operational practice of these methods has not been widely undertaken because LSP acquisition and analysis are either highly specialized, time consuming, or subjective, requiring

* Corresponding author. Tel.: +1-613-520-2600; fax: +1-613-520-4301.
E-mail address: doug_king@carleton.ca (D.J. King).

0034-4257/02/$ - see front matter © 2002 Published by Elsevier Science Inc.
PII: S0034-4257(02)00050-0

specially trained personnel and equipment (King, 2000). Thus, methods to automate and simplify acquisition and analysis are required for an effective remote-sensing-based assessment methodology.

Potential improvement of the utility of remote sensing for regeneration assessment may be obtained through the application of automated tree detection–delineation algorithms. Estimates of tree spatial pattern, tree abundance, crown size, and canopy structure can be made given accurate detection and delineation of crowns. Isolation of individual trees also provides for improved species classification through analysis of within-crown spectral data (Gougeon, 1998), spatial data (Haddow, King, Pouliot, Pitt, & Bell, 2000), and crown shape (Brandtberg, 1998). Further, crown dimensions can be used to model tree structural variables (e.g., stem diameter, height, and biomass) useful in forest inventory and evaluation of growth success (Culvenor et al., 1998; Hayward & Slaymaker, 2001).

Automated tree detection and crown delineation algorithms developed to date have been applied almost entirely in mature forest conditions. A summary of these is given in the next section with details of the forest conditions in which they were developed and tested. Some algorithms work well in relatively closed canopies, while others are more suited to individual trees with little crown overlap and full rounded crowns. Most have been developed for imagery of 0.5- to 2-m pixel spacing, which in mature forests, results in crown diameter:pixel spacing ratios of less than about 8:1. In remote sensing of young regenerating trees, however, Pitt et al. (1997) concluded that only the very high-resolution capabilities of aerial photography and digital cameras would be suitable. In this paper, a detection–delineation algorithm is presented and evaluated using airborne imagery of 5- to 15-cm pixel spacing and 6- to 10-year-old conifer trees planted at 1-m spacing. In these conditions, the crown diameter:pixel spacing ratio is about 17:1 and individual tree crowns are well resolved with a large number of pixels and high data variance within each crown. The algorithm was designed specifically to improve upon current tree detection algorithms by identifying and removing false positives corresponding to resolved branch clusters within a crown, and to accurately detect crown boundaries while avoiding within-crown shadow edges.

2. Objectives

The objectives of this research were to:

1. Develop a tree detection and delineation algorithm for very high resolution remote sensing of regenerating coniferous forests.
2. Conduct a detailed evaluation of the accuracy of the algorithm against field data of known tree locations and crown diameters.

3. Previous research in tree detection and delineation

3.1. Tree detection and delineation algorithms

At present, detection and delineation algorithms are based on two distinct spectral properties of tree crowns: the association of a tree apex with a local maximum image brightness value, and delineation of the crown boundary by local minima brightness values. Visually, this spectral crown structure is analogous to that of an upward pointing cone or mountainous shape when viewed in three dimensions. Approaches to tree detection have attempted to identify local maxima using (1) enhancement and thresholding (Dralle & Rudemo, 1997; Walsworth & King, 1998) where a global image operation such as smoothing or high-pass filtering is applied and the resulting pixel brightness values within a defined range are extracted as estimates of tree locations, (2) template matching (Pollock, 1998) involving the correlation between a geometric–radiometric tree crown model and image data, (3) multiscale analysis (Brandtberg & Walter, 1998) where the occurrence of edges over several image scales is examined to define a region in which the brightest pixel value is taken as the tree apex, and (4) local maximum filtering (Culvenor, Coops, Preston, & Tolhurst, 1998; Gougeon, 1997; Niemann, Adams, & Hay, 1998; Wulder, Niemann, & Goodenough, 2000) where the maximum pixel brightness value in a moving-window sample of a specified size is taken to represent the tree apex. Tree delineation has been accomplished by (1) outlining a network of minimum image values, known as valley following (Gougeon, 1995); (2) region grouping (Brandtberg & Walter, 1998; Walsworth & King, 1998), involving the identification of groups of similar neighbouring pixels; and (3) a combination of these two (Culvenor et al., 1998).

Specifically in this research, variable window local maximum filtering methods identified by Wulder et al. (2000) were expanded to improve detection and provide for automated crown delineation. With local maximum filtering, a moving window is passed over the image and the location of the maximum value in each window is recorded. These windows can be overlapping or not, the nonoverlapping requirement ensures that pixels in the image are evaluated within only one sample window frame, reducing detection error caused by portions of bright trees being repeatedly detected with overlapping windows. However, with either moving-window strategy, accurate results are dependent on the identification of an appropriate sample window size. Large windows result in missed trees (omission error) because the window contains multiple tree apexes. With small window sizes, too many apexes are identified (commission error) because the small window does not always contain a true tree apex. Wulder et al. addressed this problem by creating variable window sizes for local maximum evaluation. The size of the window was based on either the range from a semivariogram or the local slope break (inflection point or a sign change in the second

derivative) for the average of eight radiometric transects extending outward from the pixel being processed. The approach taken in this research is conceptually similar, but is mechanically different in (1) the analysis of transect data (maximum rate of change rather than inflection point), (2) creating a circular rather than square sample window, and (3) the use of a greater number of transects (up to 360 if desired).

3.2. Tree detection and delineation accuracy assessment

Evaluation of these algorithms is typically based on individual tree or aggregated assessments. Individual assessments compare automated and reference data for single trees, whereas aggregation averages automated and reference data within a given area for comparison (e.g., the number of trees detected per hectare). Accurate individual evaluations are preferred as more detailed information is provided for decision making/analysis; however, this is difficult to achieve. Aggregated estimates generally result in higher accuracies than individual estimates as errors of omission and commission in tree detection, or overshoots and undershoots in crown boundary delineation tend to be averaged out in the aggregation process.

Tree detection accuracy has been well researched and is commonly performed at an individual tree level using reference data consisting of tree locations visually interpreted from the imagery (Brantberg & Walter, 1998; Gougeon, 1995; Niemann et al., 1998; Pollock, 1998; Walsworth & King, 1998). For example, Gougeon (1995) found that the total number of correctly identified trees in a mature forest plantation ranged between 35% for red pine and 85% for a mixed stand of red pine and white spruce. Comparisons with field data (Brandtberg & Walter, 1998; Wulder et al., 2000) are less common due to the difficulty and associated costs of identifying tree locations in the field. One example is presented in Wulder et al. (2000) who, working in natural and plantation forests, reported a best result of 62% correctly identified trees with 11% commission error using a variable window detection algorithm. Comparing automated and field estimates at an aggregated level is more feasible (Gougeon, 1995; Gougeon & Leckie, 1998), as only the number of trees in the plot is required, not their exact location. However, the number of missed and falsely identified trees cannot be evaluated for algorithm testing and refinement. This type of evaluation was used by Gougeon and Leckie (1998) to determine the accuracy of a valley-following algorithm applied to several species and age classes of forest regeneration. Results showed that average error for the different conditions ranged from 43% to 11% for 7- and 8-year-old jack pine stands, respectively.

Tree delineation accuracy has not commonly been evaluated because of the difficulty of precisely measuring tree crowns in the field. Field-based crown measurements are subject to errors relating to how well field personnel can project the crown boundary down to a measuring device and identification of a suitable boundary point to measure for tightly overlapping or irregular crowns. Instead, studies in natural forests have commonly used crown diameter to evaluate delineation accuracy. Pollock (1998) evaluated crown-diameter accuracy for individual trees, but results were only compiled for dominant tree crowns. More importantly, the template-matching algorithm that was evaluated does not actually delineate the crown, which is required to isolate spectral data for enhanced species classification. Brandtberg and Walter (1998) evaluated crown-diameter accuracy for plot-level data and found no relation between the automated and ground estimates. Culvenor et al. (1998) validated a delineation algorithm using crown area and simulated forest imagery where defined crowns of known area served as the reference data. In conifer forest regeneration conditions, small tree sizes provide an ideal means to evaluate delineation accuracy as individual trees can be more easily identified in the field and crown-diameter measurements can be made quickly and with greater precision than in mature forests. However, only one study to date has conducted such validation. Gougeon and Leckie (1998), using a hybrid delineation algorithm based on Gougeon's (1995) original valley-following approach, found an aggregated study-wide error in average crown diameter of 8.5%, but it was also determined that the 30-cm pixel spacing was too large to detect and delineate the smaller trees present.

A critical factor found to affect all tree detection and delineation algorithms is within-crown brightness variation. In high-resolution imagery, within-crown variation is large due to the effect of branches and branch shadow patterns on the spectral response of the crown. This causes crowns to deviate from the conic shaped model, making detection and delineation more complex. Decreasing the image resolution averages spectral data over a larger areal unit and reduces this effect. However, at lower image resolutions crown boundaries become less distinct, making them harder to identify (Fig. 1).

To characterize the generalization of crown shape at different image resolutions we propose the use of a one-dimensional ratio of the average crown diameter to the pixel size or the range of crown diameter to pixel size ratios for the range of crown sizes in a study. For example, in Fig. 1 this ratio is approximately 19:1 and 6:1 for the large crown and 8:1 and 3:1 for the smaller crown at the high and low image resolution, respectively. It is evident from this example that ratios below 3:1 do not retain distinct crown boundaries and ratios above or near 19:1 may contain too much within-crown variation for accurate delineation. Thus, this ratio can be used as a guide to determine the most appropriate image resolution to use for detection/delineation based on an estimate of the average crown size or expected range of crown sizes (e.g., 95% bounds) in the study area. To date, with the exception of Brandtberg and Walter (1998), average crown diameter to pixel size ratios have typically been small (e.g., about 10:1 in Gougeon, 1995; 5:1

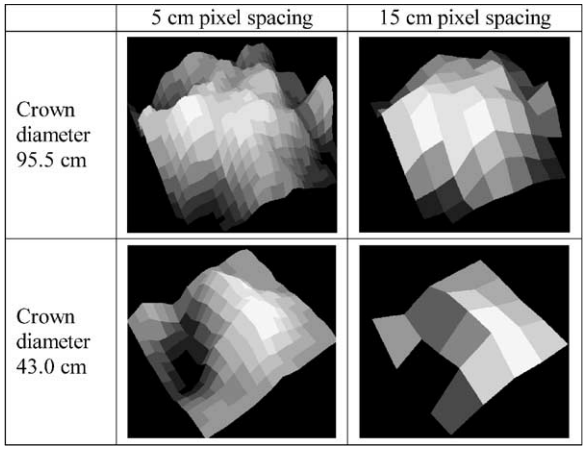

Fig. 1. Three-dimensional view of large and small tree crowns in the near-infrared band for pixel sizes of 5 and 15 cm. This figure illustrates the greater within-crown variability of large crowns with the 5-cm pixel size and the less distinct crown boundary of smaller crowns at the 15-cm pixel size.

in Culvenor et al., 1998; 4:1 in Gougeon and Leckie, 1998). The optimum ratio for a given algorithm will also be dependent on its sensitivity to within-crown variation and boundary brightness gradient. However, reporting the ratio in tests is very useful, as it allows for comparison of algorithm performance over a range of ratios and for comparison of studies of similar ratios conducted in different forest conditions.

4. Methods

4.1. Study area

The study area consists of an experimental arboretum located outside of Sault Ste. Marie, Ontario (46°33′ N, 84°27′ W), established in 1994 as part of an ongoing effort to identify the effects of various levels of vegetative competition on black spruce (*Picea mariana* [Mill.] B.S.P.) and jack pine (*Pinus banksiana* Lamb.) crop trees. The site is arranged into three blocks based on soil properties: sand, clay, and loam. Each block contains ten 42 × 14-m subplots of key competition species established at several densities. Crop species (spruce and pine) were established at a constant spacing of 1 m in all subplots. In this study, to minimize the effect of known error sources on the detection and delineation algorithm, the selection of suitable subplots was constrained by three factors. First, subplots with competing deciduous species were removed to prevent detection/delineation error occurring from the effect of overtopping competition masking the spectral characteristics of the crop trees. Second, only image data within 7° of nadir were extracted to avoid variations in shadow–crown geometry across the image caused by the nonvertical position of the sun and variable optical view angle. The seven-degree requirement was selected based on an in-depth analysis of radiation geometry conducted for mature forests by Culvenor (2000). Third, only the subplots containing spruce crop trees were used, as intense intraspecific competition in jack pine subplots rendered individual crowns unidentifiable in the imagery. In total, eight subplots (198 trees) were extracted from the loam, sand, and clay blocks and used to create the image subset for analysis. In previous research at the site, Haddow et al. (2000), using 2.5-cm pixel colour infrared digital camera imagery, were able to automatically classify and count these conifers at age 2 years (1996) in the low- to no-competition plots (similar to a leaf-off condition) with over 90% accuracy, and to model cover and leaf area index of competing vegetation with standard errors of 10–20%.

4.2. Ground data

For validation of crown delineation, crown diameters were measured in late summer 1999 by Ontario Ministry of Natural Resources staff. Measurements were made in N–S and E–W directions at the crown base of the inner 25 trees in each subplot and the arithmetic average taken to provide a single summary value for comparison with image delineations. Crown diameters ranged from 16 to 145 cm with a mean of 85 cm (Fig. 2). For validation of detection results, tree positional data were not required, as the initial planting arrangement of 1-m spacing was known and is identifiable in the imagery.

4.3. Image data

Images of the study site were acquired in a leaf-off condition on April 25, 2000 between 12:00–14:30 h using a Kodak DCS 460 CIR digital camera. Over this period, the sun zenith angle ranged from 52° to 56°. Three spectral bands were acquired in the green (500–600 nm), red (570–780 nm), and near-infrared (NIR, 710–800 nm). To achieve the desired 5-cm pixel spacing, a flying height of 196.6 m

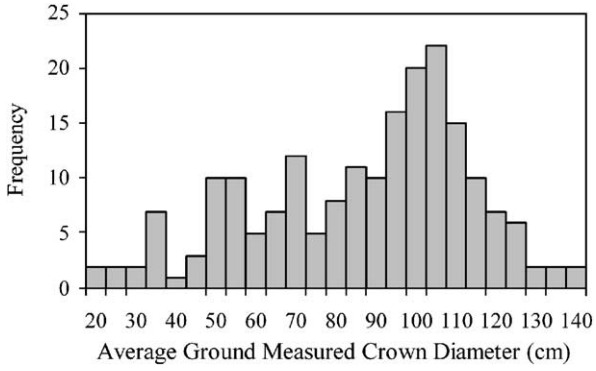

Fig. 2. Histogram showing the distribution of field-measured crown diameters (average of N–S and E–W directions for each tree) used in the analysis.

and lens focal length of 35 mm were used. The shutter speed was set at 1/4000 s to optimize spatial detail and exposure, and to minimize image motion (approx. 1/4 pixel in each exposure).

4.4. Tree detection and delineation algorithm

4.4.1. Detection

The algorithm developed in this study consists of two separate programs, one for detection and one for delineation. Together these programs are referred to as 'local maximum refinement and delineation algorithm' or LMRDA. The tree detection phase consists of the seven steps denoted A to G in the following description and in Fig. 3. In the first stage (A), image preprocessing is undertaken to enhance crown apex (or local maximum) distinctiveness, minimize the amount of bright crown non-apex pixels, and suppress the spectral response of bright soil in the imagery for tree detection. Amongst several processing types tested, including common vegetation indices, the best results were obtained using an absolute difference image of the NIR and red spectral bands. A moderate amount of Gaussian smoothing (filter size = 11 × 11, $\sigma = 5$) is also applied to simplify crown form and reduce image noise (Fig. 4).

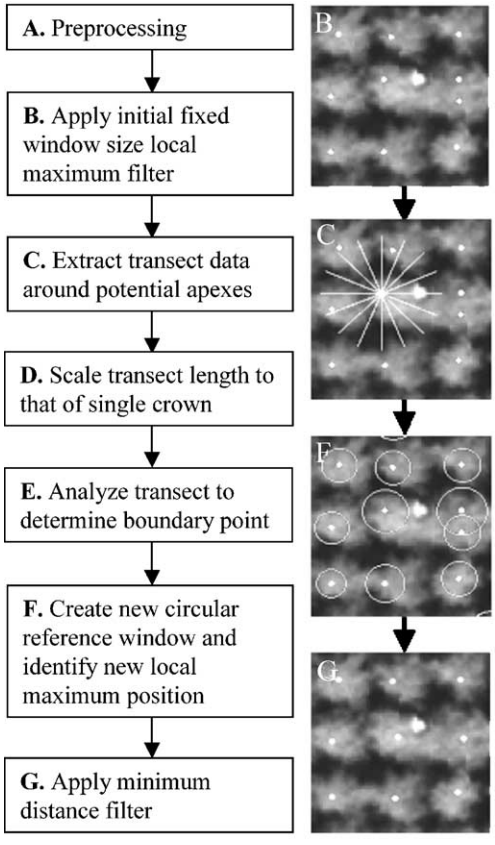

Fig. 3. Overview of tree detection algorithm process. Stages of the algorithm are lettered A–G. On the left is the complete process, on the right are images representing output at critical stages (note stage letter in upper left of each image).

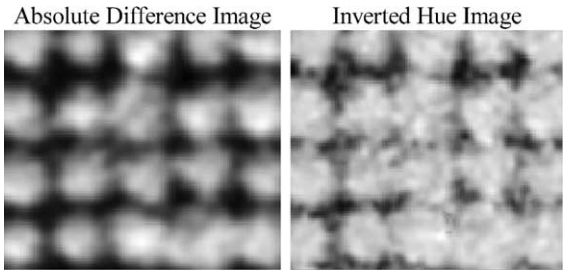

Fig. 4. Example images showing image preprocessing for optimal detection and delineation: absolute difference image used in crown detection (left), and inverted hue image used in crown delineation (right).

In stage (B) a nonoverlapping local maximum filter is applied to the image. The window size is specified by the user, but should be small compared to the average crown size in the image, as the algorithm only works to reduce the occurrence of commission errors. In this study, window sizes of 15 × 15 to 30 × 30 pixels were evaluated.

In the third stage (C) image data surrounding a potential tree apex are extracted using the transect sampling scheme depicted in Fig. 3C. The number of transects used in the analysis is selected by the user and can be set as high as 360 and as low as 4. Using more transects can improve results; however, the improvement saturates quickly as a reasonable crown radius for detection purposes can be estimated with approximately 15–20 transects. Further, the use of more transects requires significantly more processing time. The initial transect length used to extract image data is defined by the user, but should be set so that it is larger than the largest expected crown radius in the image.

Transect scaling, determining the best transect length for tree edge detection, is accomplished in stage (D). The transect data are modelled with a fourth-order polynomial and data from the end of the transect are iteratively removed one pixel value at a time until a user-defined r^2 value is reached for the original and modeled data. This process provides a good generalization of the image data while appropriately scaling the transect to be slightly larger than the actual crown radius. Fig. 5 shows how the initially extracted transect data are reduced to a suitable length for crown-edge detection using the r^2 value from a fourth-order polynomial fit. The choice of the r^2 cut-off depends on the variability of the data and pixel spacing. At large pixel spacings, a small number of transect pixel values are extracted. Thus, using high r^2 values (0.95) may leave too few remaining values for crown-edge detection if some are removed in this process. Similarly, in the case of noisy data or data with high variability, using a high r^2 value can result in a large amount of transect data being removed in order to achieve the desired polynomial fit. Smoothing with a low-pass filter as in stage (A) can be an effective means to reduce image noise allowing for higher r^2 cut-off values to

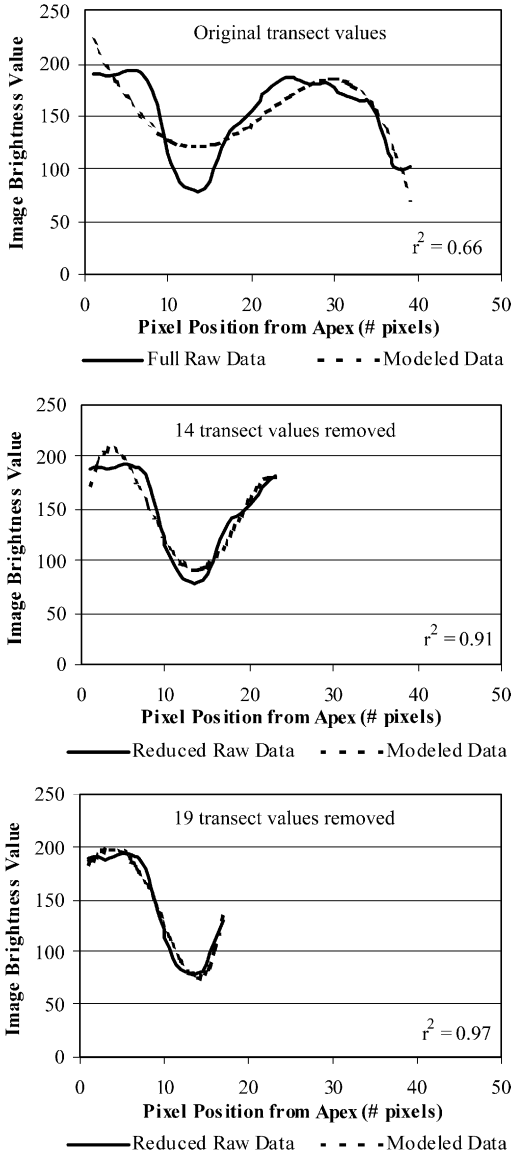

Fig. 5. Example of transect scaling process, (Stage D of the algorithm). The top figure shows the full transect length while the bottom figure shows the reduced transect length determined using a best fourth-order polynomial model fit criterion ($r^2 = 0.95$).

be used. In this study, user-specified r^2 thresholds ranged from 0.90 to 0.98 depending on the image pixel spacing.

In the fifth stage (E), the crown radius for each transect is estimated by examining the modeled data of the reduced transect to identify the maximum rate of change in the transect image values. The maximum rate of change is an edge-detection operator that is calculated by sequentially subtracting transect brightness values from the preceding value and taking the maximum of these values as the detected edge (i.e., maximum value in the first derivative for a defined set). The use of the maximum rate of change position requires appropriately scaled transects (from Stage D) so that the most significant boundary (highest rate of change) identified is indeed that for the crown under consideration and not for a more abrupt edge of a neighbouring tree. Inflection points (the change of sign of the second derivative) were also tested for this stage of the algorithm but were rejected because there were often more than one identified for a given transect, representing small within-crown edges.

Circular reference windows are created in stage (F) by estimating the crown radius based on the average distance from the apex to the crown boundary identified in stage (E). However, before averaging, extreme values are removed by converting distance estimates to Z score values and removing values greater than 2 (representing data that do not fall within 95% of the mean). Z scores are calculated as:

$$Z = (X_i - X)/s$$

where X_i is the distance to the most significant edge of transect i, X is the mean distance, and s is the standard deviation for the distances. The remaining distances are averaged to define a radius for the new circular reference window. The spectral data within each of the newly defined circular windows are then examined to determine the local maximum value, which is taken as the final tree location.

In the final stage (G), a minimum distance filter is applied that returns the centroid of a group of pixels identified as local maxima in the previous steps that occur within a user-defined distance of a point, a procedure similar to that developed by Culvenor (2000). The purpose of the filter is to remove apexes that occur closer together than the physical structure of the trees in the image would allow.

4.4.2. Delineation

Image preprocessing for delineation was different from that applied for detection. To enhance the image spectral properties for tree delineation an inverted hue image (Fig. 4) was used, as it provided a useful spatial gradient for crown-edge detection and maintained the distinct crown structure on the shaded side of the crown. The absolute difference image used for detection was not useful in delineation as it masked the spectral response on the shaded side of the crown causing crown boundaries to be underestimated. Gaussian smoothing was also applied to reduce image noise (filter size = 11×11, $\sigma = 5$).

The delineation component of the LMRDA is based on the same design as the detection program, but returns the position of the crown edge for each transect rather than the distance to the edge. If the distance for a detected edge is smaller than a user specified minimum edge distance the point is removed. The remaining edge points are then used to construct a polygon representing the crown boundary. In this study, the minimum edge distance used was 1 pixel.

In some cases, the delineated polygon can be improved by removing unlikely internal and external angles. In the case of spruce trees, the round crown shape makes acute polygon angles unlikely and, therefore, they should be removed. Fig. 6 shows the effect of sequentially removing

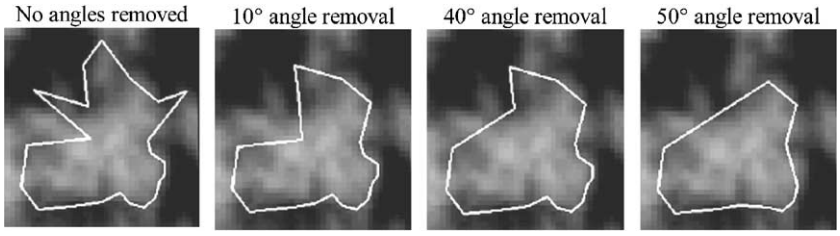

Fig. 6. Effect of removing points that cause extreme internal polygon angles in delineated crowns.

larger polygon angles. Without angle removal, the delineated polygon appears to be most similar to a natural crown shape, but it has some extended points and rapid indentations that do not match the crown boundary. Applying the 40° polygon angle removal reduces the presence of these points providing a generalized representation of the crown shape. Determination of the most suitable angle removal is left to the user; in this study angles of less than 20° were removed. However, if trees have large branches, it may be necessary to include polygon angles of less than 20° in order to make rapid directional changes in following the crown boundary. The choice of the size of the angle to filter is in part related to the number of transects used in generating the polygon. With more transects, larger polygon angles can be removed, as several polygon vertices should survive the filtering process. When using a smaller number of transects, care must be taken not to remove too many points as the polygon shape may be dramatically altered if not removed completely.

4.5. Detection and delineation algorithm evaluation

The tree detection and delineation algorithms were tested separately so that the error of each could be assessed independently on an individual tree basis and for aggregated data.

4.5.1. Detection accuracy

Detection accuracy was assessed by comparing a truth map based on prior knowledge of tree locations (experimental design) and detected apexes. For each known tree, a single detected apex within the boundary of the crown was chosen to represent the crown and the remainder, if any, were counted as commission errors. Commission error was also counted when a local maximum point identified an image object other than a tree crown. Omission errors were counted when no apex was detected within the boundary of a known crown. The detection algorithm accuracy was compared to accuracies produced by ordinary local maximum filters (with no additional refinement) for fixed-window sizes ranging from 3×3 to 30×30 pixels. Besides errors of omission and commission, overall accuracy of each detection method was defined as:

$$\mathrm{AI}\ (\%) = [(n - (\mathrm{O} + \mathrm{C}))/n] \times 100$$

where AI is an accuracy index in percent, O and C represent the number of omission and commission errors, and n is the total number of trees in the image to be detected. The purpose of the index is to count all error against the correct number of trees to be detected. This provides a single summary value for comparison of detection results.

4.5.2. Delineation accuracy

For each delineated tree crown, dimensions were extracted in the same two directions as the ground data using a program written to measure the delineated polygon diameter starting from the polygon centroid determined using the minimum bounding box method. These two values were averaged (arithmetic) and compared with the average ground-diameter estimates. In addition, tree crowns were manually delineated by the first author from the screen display of the original 5 cm imagery and their resulting diameters were compared to the ground data. To evaluate the individual crown measurement error, the root mean square error (RMSE) of the crown diameters as a percentage of the mean true diameter was calculated as:

$$\mathrm{RMSE}\ (\%) = 100 \times [((\Sigma(I_i - G_i)^2)/n)^{0.5}]/G$$

where G_i are the ground diameter measurements, G is the mean value of ground diameters, I_i are delineated crown

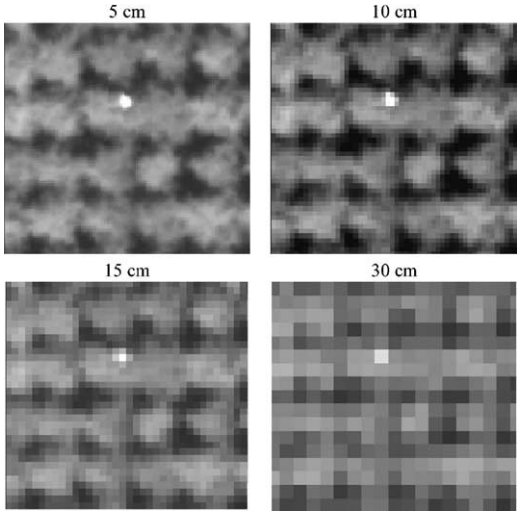

Fig. 7. Example images showing the results of resampling to pixel spacings of 10, 15, and 30 cm from the original 5-cm pixel spacing.

Tables 1
Results of tree detection for several ordinary local maximum filters with fixed-window sizes (15 × 15 to 30 × 30 pixels) and for the LMRDA at each of the pixel spacings studied (5 to 30 cm)

5-cm pixel spacing	15 × 15	20 × 20	25 × 25	30 × 30	LMRDA
Commission (%)	33.3	10.1	6.1	2.5	10.1
Omission (%)	1.0	1.0	15.7	39.9	1.0
Accuracy index (%)	65.7	88.9	78.3	57.6	88.9
10-cm pixel spacing	**7 × 7**	**10 × 10**	**13 × 13**	**16 × 16**	**LMRDA**
Commission (%)	54.5	13.6	7.6	2.5	9.1
Omission (%)	1.0	3.0	17.2	43.9	2.0
Accuracy index (%)	44.4	83.3	75.3	53.5	88.9
15-cm pixel spacing	**5 × 5**	**7 × 7**	**9 × 9**	**11 × 11**	**LMRDA**
Commission (%)	38.4	9.1	2.5	0.0	3.0
Omission (%)	2.0	5.1	22.7	40.9	6.1
Accuracy index (%)	59.6	85.9	74.7	59.1	90.9
30-cm pixel spacing	**3 × 3**	**4 × 4**	**5 × 5**	**6 × 6**	**LMRDA**
Commission (%)	58.1	16.7	6.1	4.5	14.6
Omission (%)	2.5	9.6	31.8	50.0	5.1
Accuracy index (%)	39.4	73.7	62.1	45.5	80.3

diameters, and n is the number of observations. To evaluate aggregated error on a stand level the mean differences between the ground and delineated crown diameter measurements were calculated by subtracting the average of the two measurements (ground — automated; ground — manual) for the entire data set and expressing these differences as a percentage of the mean of the ground data. Scatterplot analysis, of the absolute difference between image and ground-measured crown diameters (y-axis) versus ground-measured crown diameter (x-axis), was also conducted to identify the systematic and random error components for a given delineation.

To determine the influence of image resolution on detection and delineation accuracy, the original untransformed imagery was resampled by averaging pixels within 2×2, 3×3, and 6×6 sample windows to produce image pixel spacings of 10, 15, and 30 cm, respectively (Fig. 7). This neighbourhood averaging resampling algorithm was reported by Hay, Niemann, and Goodenough (1997) to provide a better approximation of imagery acquired at a smaller scale than the more common nearest neighbour, bilinear, and cubic convolution resampling methods.

5. Results

5.1. Tree detection

As expected, with fixed sized ordinary local maximum filters, increasing the sample window size increased omission error, whereas decreasing the window size increased commission error (Table 1). The LMRDA produced lower commission and omission error than all local maximum filters tested. Its overall accuracy was better in all cases but one 5-cm pixel spacing 20×20 local maximum filter, where it produced the same accuracy index. Errors of omission and commission for LMRDA were also more balanced, not varying as widely as the fixed-window results. Thus, LMRDA provides accurate detection results and removes the difficulty of selecting the most appropriate sample window size for a local maximum filtering operation. The LMRDA detection results were not influenced by pixel spacing in the range of 5–15 cm, whereas the much larger 30-cm pixel spacing did reduce detection accuracy significantly. For visual evaluation, Fig. 8 shows the 5-cm pixel spacing results overlaid on the original imagery. A large amount of the detection error for LMRDA was due to the presence of short ground vegetation in the imagery. It had a similar spectral response to that of the conifer trees, because it had started to become green at the time of imaging. In some cases, this led to its detection as

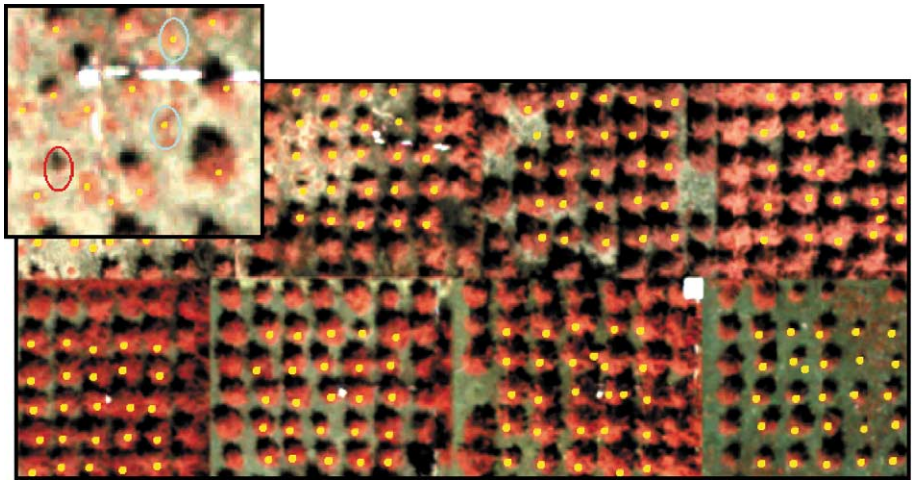

Fig. 8. Detection results using 5-cm pixel spacing imagery. The outer row and column of trees in each plot were not included in the analysis because ground diameters had not been measured. In the zoomed-in inset, cyan = commission error due to the presence of short ground vegetation and red = omission error.

Table 2
Error in average crown diameter measured from automated delineations at four image pixel spacings and for manual delineation at the 5-cm pixel spacing

Delineation/error measure	Pixel spacing (cm)/CD:PS				
	5/17:1	10/8:1	15/6:1	30/3:1	Manual 5/17:1
RMSE (%)	17.9	19.0	22.9	39.0	11.2
Mean difference (%)	2.8	2.8	−2.4	−28.4	−4.1

The crown diameter to pixel size ratio (CD:PS) is shown beside each pixel size.

an apex instead of an adjacent tree. The presence of short ground vegetation is a difficult problem, as it is hard to mask in multispectral imagery with broad spectral bands. Several classification attempts were made using grey-level co-occurrence texture measures along with spectral data in a maximum likelihood classification, but it was not possible to effectively separate it from the smaller conifer trees. A practical solution is true leaf-off imaging, just after snow-melt when only the conifers are green.

5.2. Tree delineation

Diameters determined from manual delineation best matched the ground measurements with approximately 11.2% error (Table 2). The automated method achieved a best result of 17.9% error for the 5-cm data. However, further testing with greater polygon angle removal (40°) produced a best automated delineation result of 14.5% with the smallest pixel spacing. In this case, using the higher angle removal resulted in very generalized crown shapes (more circular) whose measured diameters better matched those measured on the ground. In the field, crown diameter measured at the crown base did not include single long branches protruding from the crown or sharp indentations. It was taken as the visually representative diameter at the E–W, N–S measurement locations to avoid introduction of measurement outliers. Thus, for this study, measurement of diameters from more generalized crown delineations better matched the field measurement technique. Decreasing image resolution also increased delineation error nonlinearly. The difference between the 5- and 10-cm image delineation was not significant (Bonferroni multiple comparison test, $P=1.00$), while increasing the pixel spacing to 15 cm resulted in greater overestimation of the crown diameters. At 30 cm, delineation error became extreme (Fig. 9). This is an expected result, as larger pixels tend to artificially increase image crown diameters due to the averaging of the spectral radiation over a larger areal unit. Fig. 9B most clearly shows this effect where the 15-cm pixel delineation error follows the same trend as the 5-cm, but is consistently larger throughout the diameter range. The results from the 15- and 30-cm resolution delineations were significantly different from those using 5-cm imagery ($P=.01$, $P=.00$, respectively). The 10-, 15-, and 30-cm delineations were also significantly different from each other ($P<.03$). Aggregating the individual tree results to average error for the study ("mean difference %" in Table 2); substantially reduced

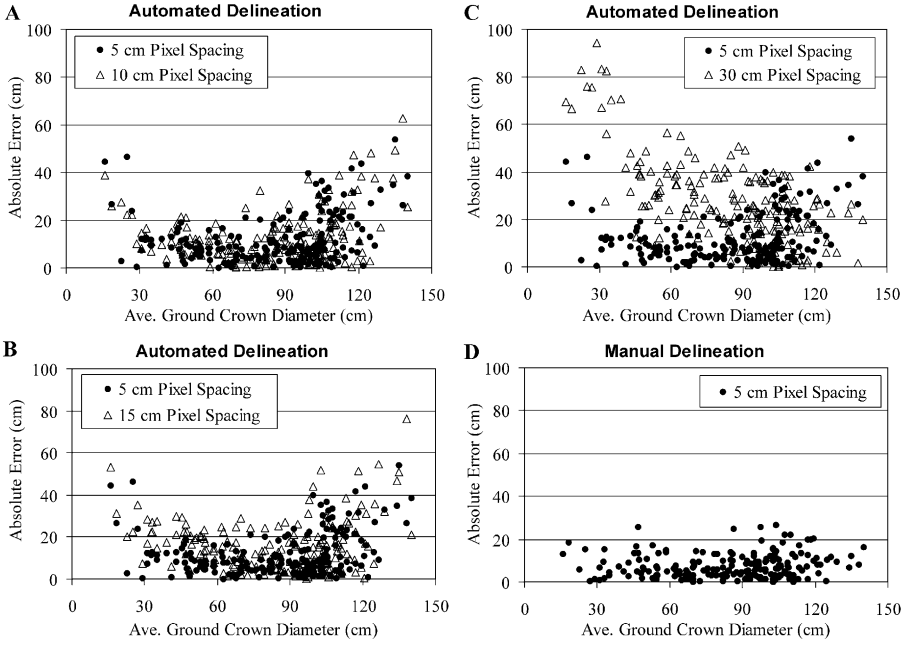

Fig. 9. The relation between absolute error in crown diameter measured from LMRDA-delineated crowns and ground-measured crown diameter for (A) 5- and 10-cm pixel spacings, showing little overall difference, (B) 5- and 15-cm pixel spacings, showing similar trends but greater error over all diameters for the 15-cm data, (C) 5- and 30-cm pixel spacings showing gross overestimation of small crowns in the 30-cm data, and (D) manual delineation showing no apparent error trends.

error as overestimates and underestimates balanced each other in the averaging process. For the 5- to 15-cm pixel spacings, aggregation reduced error from 17.9–22.9% to 2.4–2.8%. In addition, the average error of each of these automated delineations was less than that of the manual delineation.

For visual evaluation, the automated method using 5-cm pixel spacing and manual delineation results are presented in Fig. 10. Comparison of the manual (cyan) and LMRDA (yellow) delineations by this means shows that plots with larger crowns (more crowded conditions identifiable in the imagery) resulted in the greatest disagreement between methods.

Examination of the individual errors revealed that the automated methods overestimated small and underestimated large crown diameters. Overestimation of the small crown diameters, similar to detection results, was due to the presence of short ground vegetation in close proximity to the crown boundary. In the case of large trees, errors were due to overlapping crowns, causing crown boundaries to be less distinct than the within-crown spectral variance. As the image resolution was degraded, the within-crown variance was reduced leading to improved delineation of larger crowns (Fig. 9C). However, at the largest pixel size of 30 cm, small crown boundaries were heavily distorted resulting in extreme overestimation of their diameters. Manual delineations did not suffer from any apparent estimation bias, producing a consistently low error across the range of diameters tested (Fig. 9D).

Based on Fig. 9A, it appears that the algorithm is most accurate within a range of crown diameters of 30–100 cm assuming a spatial resolution of 5–10 cm. This represents 63% of the originally sampled trees. Using observed values within this range improved the individual delineation results (Table 3). The largest improvement in accuracy was for the 5-cm pixel spacing reducing error from 17.9% to 14.0%. However, as resolution degraded, the improvement decreased or resulted in greater error than that of the full range, suggesting that the 30- to 100-cm crown diameter range was most suited to the 5-cm pixel spacing (15:1 average crown diameter to pixel ratio). The manual delineation remained approximately the same, as the crowns were well delineated over the full crown-diameter range and the manual interpreter was better able to identify the crown edge in the presence of short ground vegetation. Contrary to the full-diameter-range evaluation, the aggregated mean difference values for the delineations are noticeably different. For the reduced diameter range, all delineations overestimate the ground-measured crown diameters. The smaller mean difference values presented earlier are due to the cancelling effect of the over- and underestimation of small and large crowns outside the optimal range examined here. Reducing the range of diameter sizes removed the cancellation effect revealing this trend.

Table 3
Delineation accuracy for crown diameter range of 30–100 cm with outliers caused by short ground vegetation removed

Delineation/error measure	Pixel spacing (cm)/CD:PS				
	5/15:1	10/7:1	15/5:1	30/2:1	Manual 5/15:1
RMSE (%)	14.0	15.8	21.5	47.4	11.7
Mean difference (%)	−3.1	−4.9	−12.9	−39.8	−6.0

The crown diameter to pixel size ratios (CD:PS) have been modified from Table 2 to reflect the data used in this subsample.

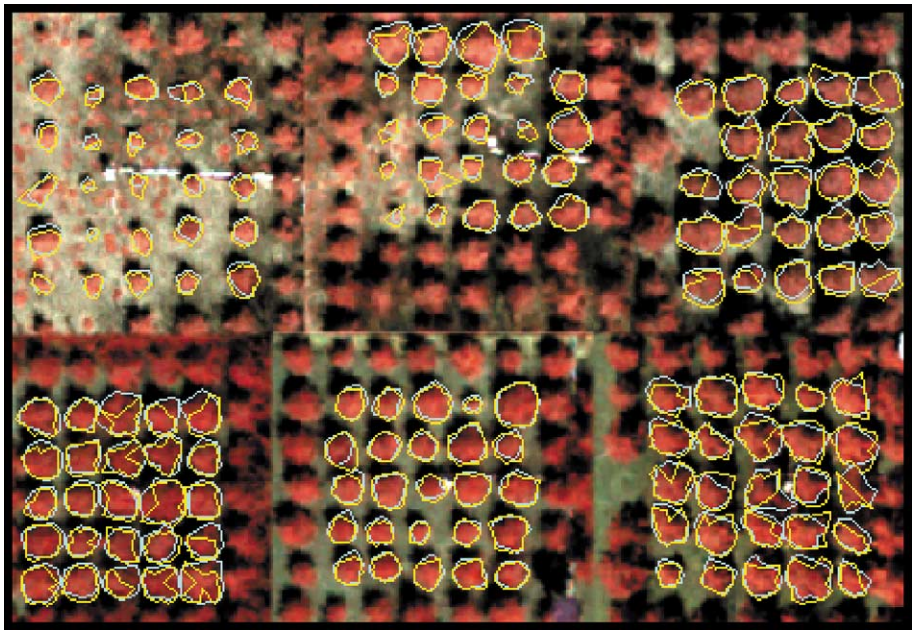

Fig. 10. Example delineation results of LMRDA (yellow) and the manual method (cyan) using 5-cm pixel spacing.

6. Discussion

The LMRDA produced better tree detection accuracies than the fixed-window local maximum filters in all cases but one where they were equivalent. Detection accuracy was high, to within 90%, for the well-controlled conditions studied. Results were also invariant to small changes in pixel spacing (5–15 cm), but larger pixel spacing caused significantly greater error. Crown delineation was more sensitive to changes in pixel spacing than crown detection. The smallest pixel spacing (5 cm) produced the most accurate diameter estimates (17.9% error), while larger spacings increased delineation error in a nonlinear manner. The most critical factor found to affect the delineation algorithm performance was the relative distinctiveness of the crown boundary in relation to within-crown variation. If within-crown variation is high and crowns are not overlapping, accurate results are likely to be obtained because the crown and background will be the most significant edge in the transect. However, in overlapping conditions, the within-crown variability can be more distinct than the boundaries, causing delineation error. In this case, the solution is to reduce within-crown variation. This requires estimation of the optimal image pixel spacing, as larger spacings reduce within-crown variation, but also decrease the distinct spatial gradient used in delineation. Heuristic estimation of optimal pixel size for delineation can be based on previous studies in which crown size to pixel ratios have been calculated. In this study, the optimum average crown size to pixel ratio was found to be 15:1. Ratios below 15:1 (fewer pixels per crown) did not improve results as the within-crown variability remained stable, but the crown boundary distinctiveness was reduced, leading to greater error. Ratios larger than 15:1 (more pixels per crown) were heavily influenced by within-crown variation, also resulting in substantial error.

For some forest management decisions, aggregated diameter measurements are required for a given management unit. In this study, aggregating individually measured crown diameters to the mean diameter of the sampled trees for the whole study reduced the error between automated and ground-measured crown diameters to less than 3%. Such areal averages may be useful as part of an initial flagging system to identify areas that are unlikely to meet future free-to-grow status, or in stocking estimation, although species composition must typically first be determined.

An important advantage of tree delineation is the potential to model tree structural variables such as tree height, stem diameter, and biomass. In this study, preliminary results of LMRDA delineated crown diameters showed strong relations with tree height (r=.86), stem diameter (r=.78), and biomass (r=.97) suggesting the potential to estimate these values using image based crown diameter estimates. On an individual assessment level it is unlikely that sufficiently accurate models could be obtained for prediction, but aggregating individual results from models could lead to reasonable area-based tree structural estimates useful in evaluating the growth success of crop trees.

The primary error sources in crown delineation that were identified in this study were crown overlap and the presence of short ground vegetation. The LMRDA algorithm produced good results even when crown overlap was significant, but errors did increase with increasing overlap. One reason for this is that the reference data consisted of diameters measured at the crown base while the delineated diameters were measured in imagery taken from above. As crown overlap increases, the delineated crown edge in the area of overlap is at progressively higher positions in the crown and not at the base. Thus, there is a greater mismatch of these two data types with increasing overlap. Crown overlaps in this study were also greater than would be expected in a 6-year-old plantation because the well-controlled 1-m tree spacing was closer than typical operational spacings of 1.5–2 m. Thus, the algorithm can probably provide similar results to those presented in this paper for plantations up to approximately 8–10 years old. In naturally regenerated forests or planted forests, a more random spacing will occur with greater variability in crown sizes and crown overlap. This could lead to detection–delineation error if crown size variability is too large to be encompassed by a single optimal pixel spacing. Evaluation and modification of the proposed algorithm to natural regeneration conditions will be an important aspect of future work, as only a small portion (maximum 18%) of forest regeneration resulting from fire and harvesting consists of plantations (Natural Resources Canada [NRC], 2000).

The presence of short ground vegetation in the imagery presented problems for both the detection and delineation algorithms due to its similarity in spectral response to tree crowns for the spectral bands analyzed. Short ground vegetation reestablishes itself quickly after snow melt, making it difficult to acquire images without its presence. Masking the response of short ground vegetation may require the development of an explicit algorithm to examine imagery for crown and shadow components, as short ground vegetation does not have an associated shadow. Alternatively, experimentation with advanced classification methods incorporating image textural characteristics may also be useful.

Another important element to evaluate, which was not present in this study, is the effect of competing vegetation. If the presence of overtopping competition strongly distorts the key spectral and spatial characteristics used in detecting and delineating crop tree crowns, then automated approaches may be inappropriate for assessing such regeneration conditions with remotely sensed data. This may occur, even in leaf-off conditions, for woody competition species such as willow, birch, aspen, and alder where dense branching may obscure the underlying conifer crown. Some herbaceous species such as raspberry and fireweed may also impact delineation results. After snowmelt, residual stems of these species still retain a vertical structure that could interfere with the spectral response of lower crop tree

branches inhibiting the delineation process. Evaluation of this effect was not conducted at this stage of the research because the required subplots did not occur within 7° of nadir making it difficult to determine if detection/delineation error was due to competition or view angle effects. However, further research is planned to develop a view angle correction to provide for this analysis.

The algorithm presented in this study has not yet been rigorously evaluated against other existing algorithms. Most have been developed and applied in mature forests with smaller crown diameter to pixel size ratios. The LMRDA algorithm was designed to utilize the high spatial information in large crown to pixel size (i.e., very high resolution) imagery. Conceptually, comparison with the most commonly reported technique, valley following, reveals some advantages of LMRDA in such imagery. Both approaches require searching for local maximum or minimum brightness values in an image using a moving-window strategy. However, in tree detection, LMRDA reexamines identified local maximum values using a secondary reference window based on the surrounding spectral/spatial properties of a potential tree. Thus, if several local maxima are found in a single crown, only one should remain to represent the crown position. In valley following, the local minima used for delineation and subsequent apex detection are subject to greater error with high-resolution imagery due to the increased presence of local within-crown valleys that can result in multiple image segments being created for a single crown. A refinement procedure, such as that presented here, to ensure that only appropriate local minimum values are used in boundary delineation may help to alleviate this problem. In crown delineation with the high-resolution imagery of this study, crown boundary detection using local minimum values tended to overestimate crown edges while the position of maximum rate of change used in LMRDA was more accurate. Thus, valley following may be more suited to coarser resolution imagery and larger trees (crown diameter to pixel size ratios ranging from 3:1 to 8:1) where crown boundaries are often effectively represented by local minimum values. However, given that delineation can currently only be accomplished with a spatial precision of one pixel (until subpixel algorithms are developed), valley-following delineation of small trees such as those of this study using coarser resolution imagery, would likely result in significant relative error. High-resolution imagery also provides greater within-crown data for spectral and textural evaluation of crown condition. Further research will continue these comparative evaluations to aid in refinement of the algorithm and to provide more quantitative comparisons with other methods.

7. Conclusion

A tree detection–delineation methodology was developed for high-resolution remotely sensed imagery. It was successfully applied in leaf-off 5- to 15-cm pixel imagery of a 6-year-old regenerating forest plantation. Individual tree detection accuracy produced a best result of 91%. Delineated tree crown diameters were within 17.9% of field measurements of crown base diameters on an individual tree basis and within 3% when averaged for the study. Further research will include evaluation of view angle and vegetative competition effects on detection–delineation accuracy, and application of the algorithm in an operational cutover. These methods and additional knowledge will be integrated into a remote sensing-based methodology for free-to-grow assessment.

Acknowledgements

This research was funded by grants to D. King from the Natural Sciences and Engineering Research Council of Canada and the U.S. National Geographic Society. The Ontario Forest Research Institute and the Canadian Forest Service provided support for airborne and field data acquisition and valuable advice. Images used in the study were acquired by the Ontario Ministry of Natural Resources Data Acquisitions Branch.

References

Brandtberg, T. (1998). Algorithms for structure- and contour-based tree species classification using digital image analysis. In D. A. Hill, & D. G. Leckie (Eds.), *Proceedings of the International Forum on Automated Interpretation of High Spatial Resolution Digital Imagery for Forestry* (pp. 199–207). Victoria, BC: Canadian Forest Service, Pacific Forestry Centre.

Brandtberg, T., & Walter, F. (1998). Automated delineation of individual tree crowns in high spatial resolution aerial images by multiple-scale analysis. *Machine Vision and Applications*, *11*, 64–73.

Culvenor, D. S. (2000). *Development of a tree delineation algorithm for application to high spatial resolution digital imagery of Australian native forest.* PhD thesis, The University of Melbourne (355 pp).

Culvenor, D. S., Coops, N., Preston, R., & Tolhurst, K. G. (1998). A spatial clustering approach to automated tree crown delineation. In D. A. Hill, D. G. Leckie (Eds.), *Proceedings of the International Forum on Automated Interpretation of High Spatial Resolution Digital Imagery for Forestry* (pp. 67–80). Victoria, BC: Canadian Forest Service, Pacific Forestry Centre.

Dralle, K., & Rudemo, M. (1997). Automatic estimation of individual tree positions from aerial photos. *Canadian Journal of Forest Research*, *27*, 1728–1736.

Goba, N., Pala, S., & Narraway, J. (1982). *An instruction manual on the assessment of regeneration success by aerial survey.* Toronto, Ontario: Ontario Ministry of Natural Resources Publication (57 pp.).

Gougeon, F. A. (1995). A crown-following approach to the automatic delineation of individual tree crowns in high spatial resolution images. *Canadian Journal of Remote Sensing*, *21*, 274–288.

Gougeon, F. A. (1997). A locally adaptive technique for forest regeneration assessments from high resolution aerial images [CD-ROM]. *Proceedings of the 19th Symposium on Remote Sensing, May 24–30, 1997, Ottawa, Ontario, Canada*. Ottawa: Canadian Aeronautics and Space Institute (CD ROM Paper 275, 13pp).

Gougeon, F. A. (1998). Automatic individual tree crown delineation using a valley-following algorithm and rule based system. In D. A. Hill, & D.

G. GoodenoughLeckie (Eds.), *Proceedings of the International Forum on Automated Interpretation of High Spatial Resolution Digital Imagery for Forestry* (pp. 11–23). Victoria, BC: Canadian Forest Service, Pacific Forestry Centre.

Gougeon, F. A., & Leckie, D. G. (1998). Forest regeneration: individual tree crown detection techniques for density and stocking assessments. In D. A. Hill, & D. G. Leckie (Eds.), *Proceedings of the International Forum on Automated Interpretation of High Spatial Resolution Digital Imagery for Forestry* (pp. 169–177). Victoria, BC: Canadian Forest Service, Pacific Forestry Centre.

Haddow, K. A., King, D. J., Pouliot, D. A., Pitt, D. G., & Bell, F. W. (2000). Early regeneration conifer identification and competition cover assessment using airborne digital camera imagery. *Forestry Chronicle*, *76*, 915–928.

Hall, R. J. (1984). *Use of large-scale aerial photographs in regeneration assessments* (Information Report NOR-x-264). Northern Forest Research Centre, Canadian Forest Service, (31 pp.) Edmonton, AB.

Hall, R. J., & Aldred, A. H. (1992). Forest regeneration appraisal with large-scale aerial photographs. *Forestry Chronicle*, *68*(1), 142–150.

Hay, G., Niemann, K., & Goodenough, D. (1997). Spatial thresholds, image-objects, and upscaling: a multiscale evaluation. *Remote Sensing of Environment*, *62*, 1–19.

Hayward, C., & Slaymaker, D. (2001). Estimating the significant above ground biomass of Amazonian rain forest using low altitude aerial videography. *Proceedings of the 18th Biennial Workshop on Color Photography and Videography in Resource Assessment, Amherst, Massachusetts, May 16–18* (CD-ROM publication, In press). Bethesda, MD: American Society for Photogrammetry and Remote Sensing.

King, D. J. (2000). Airborne remote sensing in forestry: sensors, analysis and applications. *Forestry Chronicle*, *76*, 25–42.

Natural Resources Canada (NRC) (2000). The state of Canada's forests 1999–2000. *Natural Resources Canada*. Ottawa, Ont: Canadian Forest Service (ISBN 0-662-29069-0, 120 pp.).

Niemann, K. O., Adams, S., & Hay, G. (1998). Automated tree crown identification using digital orthophoto mosaics. In D. A. Hill, & D. G. Leckie (Eds.), *Proceedings of the International Forum on Automated Interpretation of High Spatial Resolution Digital Imagery for Forestry* (pp. 105–113). Victoria, BC: Canadian Forest Service, Pacific Forestry Centre.

Pitt, D. G., & Glover, G. R. (1993). Large-scale 35-mm aerial photographs for assessment of vegetation-management research plots in eastern Canada. *Canadian Journal of Forest Research*, *23*, 2159–2169.

Pitt, D. G., Wagner, R. G., Hall, R. J., King, D. J., Leckie, D. G., & Runesson, U. (1997). Use of remote sensing for forest vegetation management: a problem analysis. *Forestry Chronicle*, *73*, 459–478.

Pitt, D. G., Runesson, U., & Bell, F. W. (2000). Application of large- and medium-scale aerial photographs to forest vegetation management: a case study. *Forestry Chronicle*, *76*, 903–913.

Pollock, R. (1998). Individual tree recognition based on a synthetic tree crown image model. In D. A. Hill, D. G. Leckie (Eds.), *Proceedings of the International Forum on Automated Interpretation of High Spatial Resolution Digital Imagery for Forestry* (pp. 25–34). Victoria, BC: Canadian Forest Service, Pacific Forestry Centre.

Walsworth, N., & King, D. J. (1998). Comparison of two tree apex delineation techniques. In D. A. Hill, D. G. Leckie (Eds.), *Proceedings of the International Forum on Automated Interpretation of High Spatial Resolution Digital Imagery for Forestry* (pp. 93–104). Victoria, BC: Canadian Forest Service, Pacific Forestry Centre.

Wulder, M., Niemann, K. O., & Goodenough, D. G. (2000). Local maximum filtering for the extraction of tree locations and basal area from high spatial resolution imagery. *Remote Sensing of Environment*, *73*, 103–114.